ARTICLE
Journal of Cellular Biochemistry 114:1395–1403 (2013)

Journal of Cellular Biochemistry

Inhibition of ZEB1 Reverses EMT and Chemoresistance in Docetaxel-Resistant Human Lung Adenocarcinoma Cell Line

Jin Ren, Yitian Chen, Haizhu Song, Longbang Chen, and Rui Wang*

Department of Medical Oncology, Jinling Hospital, School of Medicine, Nanjing University, Nanjing 210002, China

ABSTRACT

Docetaxel has been used as one of the first-line chemotherapies in solid tumors including advanced non-small cell lung cancer (NSCLC). However, limited responses to chemotherapy are observed in clinic and the molecular mechanisms have not been fully understood. Emerging evidence suggests that epithelial–mesenchymal transition (EMT) plays an important role in the processes of tumor metastasis as well as resistance towards anticancer agents. In this study, it was observed that docetaxel-resistant human lung adenocarcinoma cell line (SPC-A1/DTX) was typical of mesenchymal phenotype. SPC-A1/DTX cell line has increased migratory and invasive capacity both in vitro and in vivo. Among the master EMT-inducing transcriptional factors, ZEB1 was found to be significantly increased in SPC-A1/DTX cell line. ZEB1 knockdown with RNA interference could reverse the EMT phenotype and inhibit the migratory ability of SPC-A1/DTX cells. Furthermore, inhibition of ZEB1 significantly enhanced the chemosensitivity of SPC-A1/DTX cells to docetaxel in vitro and in vivo and ectopic expression of ZEB1 increased the chemoresistance of SPC-A1 cells to docetaxel. All these results provide experimental evidence that ZEB1 might be an attractive target for the treatment of human NSCLC. J. Cell. Biochem. 114: 1395–1403, 2013.

KEY WORDS: ZINC FINGER E-BOX-BINDING HOMEOBOX 1 (ZEB1); EPITHELIAL–MESENCHYMAL TRANSITION (EMT); DOCETAXEL; CHEMORESISTANCE

Lung cancer is the leading cause of tumor-related death in the world [Parkin et al., 2005]. Non-small cell lung cancer (NSCLC), including squamous cell carcinoma, adenocarcinoma, and large-cell carcinoma, accounts for 70–80% of all lung cancers [Jemal et al., 2008]. Many lung cancer patients are already at an advanced stage when diagnosed mainly due to the late symptomatology and early distant metastases, with their therapeutic effects highly dependent on medical treatment, especially chemotherapy. Docetaxel is a semi-synthetic analogue of paclitaxel and has been used as the first-line therapeutic agent in advanced NSCLC with genotoxic effects including promotion of microtubule polymerization and inhibition of microtubule depolymerization [Wang et al., 2000]. However, NSCLC patients generally develop limited responses to docetaxel-based chemotherapies and the underlying mechanisms of docetaxel-resistance have not been fully understood [Yu, 2002].

Emerging evidence shows that epithelial–mesenchymal transition (EMT) is associated with cancer cell metastasis as well as drug resistance [Hiscox et al., 2006; Yang et al., 2006; Kajiyama et al., 2007]. Cancer cells with EMT phenotype such as lost of epithelial characteristics and acquirement of mesenchymal properties often have enhanced motility and invasive abilities [Hugo et al., 2007; Min et al., 2008]. A particular characteristic of EMT is the down-regulation of E-cadherin, which causes disruption of cell-to-cell junctions and increase of mesenchymal markers such as Vimentin, fibronectin, and N-cadherin [Larue and Bellacosa, 2005; Kong et al., 2008; Min et al., 2008]. EMT has been shown to play a crucial role in drug resistance of cancer cells against conventional therapeutics including taxol, vincristine, oxaliplatin, as well as epidermal growth factor receptor (EGFR)-targeted agents [Sabbah et al., 2008]. Activation of some transcriptional repressors including Slug/Snail2, zinc finger E-box-binding homeobox 1 (ZEB1)/δEF1, ZEB2/SIP1 and Twist, has been reported to be involved in the regulation of E-cadherin and EMT [Yang et al., 2004; Pena et al., 2005; Peinado et al., 2007; Barr et al., 2008]. Ectopic expression of these

Additional supporting information may be found in the online version of this article.

Grant sponsor: National Natural Science Foundation of China; Grant numbers: 81172106, 81172335.

*Correspondence to: Rui Wang, Department of Medical Oncology, Jinling Hospital, School of Medicine, Nanjing University, Nanjing 210002, China. E-mail: ruiwangrui@yahoo.com.cn

Manuscript Received: 22 August 2012; Manuscript Accepted: 6 December 2012

Accepted manuscript online in Wiley Online Library (wileyonlinelibrary.com): 17 December 2012

DOI 10.1002/jcb.24481 • © 2012 Wiley Periodicals, Inc.

transcription factors in epithelial cancer cells leads to a complete loss of epithelial polarity and disappearance of adherens junctions [Comijn et al., 2001; Eger et al., 2005; Vandewalle et al., 2005; Aigner et al., 2007a; Spaderna et al., 2008].

Among these master EMT-inducing genes, ZEB1, a member of zinc-finger E-box binding homeobox (ZFH) family, is considered to be a key transcriptional factor in cancer progression. ZEB1 plays a critical role in embryonic development, cell differentiation, cell cycle and susceptibility to apoptosis [Wu et al., 2005; Mejlvang et al., 2007]. Intriguingly, ZEB1 is able to bind to the promoter of E-cadherin and suppress transcriptional synthesis of E-cadherin mRNA, which is a critical marker of epithelial phenotype [Eger et al., 2005; Aigner et al., 2007b]. ZEB1 is also shown to promote EMT by decreasing the expression of cell polarity proteins, including Crumbs3, Pals1-associated tight junction protein and human lethal giant larvae homologue 2 [Aigner et al., 2007a; Shirakihara et al., 2007; Spaderna et al., 2008]. In this study, it was observed that the docetaxel resistant-human lung adenocarcinoma cell line, SPC-A1/DTX, displayed a typical EMT phenotype. The role of ZEB1 in EMT and chemoresistant phenotypes of SPC-A1/DTX cells was investigated and the underlying molecular mechanisms were also discussed.

MATERIALS AND METHODS

CELL CULTURE

Human lung adenocarcinoma cell lines SPC-A1 and H1299 were preserved in our lab and grown in RPMI 1640 medium supplemented with 10% fetal bovine serum (FBS, GIBCO), 100 U/ml penicillin and 100 μg/ml streptomycin at 37°C in a humidified, 5% CO_2 atmosphere. The docetaxel-resistant SPC-A1 cell line (SPC-A1/DTX) was established and preserved in 5 μg/L docetaxel as described previously [Feng et al., 2011]. The docetaxel-resistant H1299 cell line was generated and preserved in 20 μg/L docetaxel (unpublished data).

MORPHOLOGIC ANALYSIS

Cells were grown to 70% confluence and visualized at ×200 magnification with an Olympus microscope (Olympus America, Inc., Melville, NY). The digital images of the SPC-A1/DTX cells and parental cells SPC-A1 were randomly taken and three researchers blinded to the results were asked to compare the images for morphologic characteristics consistent with EMT.

TRANSIENT TRANSFECTION

Small interfering RNAs (siRNAs) targeting ZEB1 (designed as siZEB1, sc-38643) and control siRNAs (designed as sicon, sc-37007) were purchased from Santa Cruz Biotechnology, Inc. The whole sequence of ZEB1 was amplified using PCR with *Bam*HI and *Hin*dIII restriction enzyme cut sites on the ends to facilitate directional cloning. The PCR products were cloned into the plasmid pcDNA3.1 (Invitrogen, Carlsbad, CA) and subsequently verified by DNA sequencing to create the recombinant plasmid pcDNA-ZEB1. Cells were planted into 6-well plates (2×10^5 cells/well) and transfected with siRNA or plasmid using Lipofectamine 2000 (Invitrogen) according to the manufacturer's protocol.

CELL VIABILITY ASSAY

Cells were seeded into 96-well plates at a density of 2×10^3 cells/well and various concentrations of docetaxel (0, 10, 20, 40, 80, 160, 320, 640, 1,280 μg/L) were added. After 48 h, cell viability was determined by MTT assay as previously described [Tsang and Kwok, 2009].

FLOW CYTOMETRIC ANALYSIS OF APOPTOSIS

Cells were harvested 48 h after transfection of the siRNAs or pcDNA-ZEB1, and apoptotic rate was determined by Annexin V-FITC apoptosis detection kit (KeyGen Biotech, Nanjing, China) according to the manufacturer's protocol. Briefly, cells were collected and resuspended in 0.5 ml binding buffer containing 5 μl Annexin V and 5 μl propidium iodide (PI), and incubated for 15 min at 37°C in the dark. The apoptotic rate was examined by flow cytometry.

COLONY FORMATION ASSAY

Cells were transfected for 48 h and seeded into 6-well plates (3×10^2 cells/well). After 14 days, cells were fixed with methanol and stained with a solution containing 0.1% crystal violet and 20% ethanol. After washing and drying, visible colonies were manually counted.

RNA EXTRACTION AND REAL-TIME QUANTITATIVE PCR

Total RNA was extracted using Trizol reagent (Invitrogen) and transcribed into cDNA using a PrimeScript RT reagent Kit (Takara, Dalian, China) according to the manufacturer's instructions. Quantitative PCR was performed in ABI 7300 Thermocycler (Applied Biosystems, Foster City, CA), using the SYBR Premix Ex Taq kit (Takara). The presence of circulating tumor cells was assessed as a function of human-specific GAPDH (hGAPDH) expression relative to mouse-specific GAPDH (mGAPDH). The primers were described in Table I.

WOUND-HEALING ASSAY

Cells were grown to confluent monolayer in 6-well plates using RPMI 1640 containing 10% FBS. Then the medium was replaced with FBS-free media, and the monolayer cells were wounded with 200 μl tip. The migration of cells into the wound zone was observed

TABLE I. Primer Sequences Used for Quantitative PCR

mRNA	Primers	Expected size (bp)
E-cadherin	Forward: 5′-CATTTCCCAACTCCTCTCCTGGC-3′ Reverse: 5′-ATGGGCCTTTTTCATTTTCTGGG-3′	90
CK-19	Forward: 5′-CATCCAGGACCTGCGGGACAAGA-3′ Reverse: 5′-AGCCAGACGGGCATTGTCGATCT-3′	85
Vimentin	Forward: 5′-AGTTCAAGAACACCCGCACCAAC-3′ Reverse: 5′-CAGGAAGCGCACCTTGTCGATGT-3′	89
N-cadherin	Forward: 5′-CTTCAGGCGTCTGTAGAGGCTTC-3′ Reverse: 5′-TGCACATCCTTCGATAAGACTGC-3′	95
Slug	Forward: 5′-GGCTTGGCTGCACTGTCTGACTT-3′ Reverse: 5′-TTCATTTCCACCCTGGCACCTAC-3′	106
Snail	Forward: 5′-CCAGCTCTCTGAGGCCAAGGATC-3′ Reverse: 5′-TGGCTTCGGATGTGCATCTTGAG-3′	108
Twist1	Forward: 5′-TACCAGGTCCTCCAGAGCGACGA-3′ Reverse: 5′-TCCTCCAGACCGAGAAGGCGTAG-3′	97
ZEB1	Forward: 5′-CAAGAAACAATCAATGCTTCACC-3′ Reverse: 5′-GGTTGTTCCATCTTGATCAACCA-3′	93

(100× magnification) at the indicated time points (0, 24, and 48 h) after scraping. The distances between the two edges of the scratched cells were measured and healing rate was calculated using the following formula: healing rate = (the distance before healing − the distance after healing)/the distance before healing × 100%.

MIGRATION AND INVASION ASSAYS

Cell migration assays were performed using Transwell migration chambers (8 μm pore size; Costar) according to the vendor's instructions. Briefly, 50,000 cells were plated into the insert of the well and the wells were washed with PBS after 18 h for migration assays. The cells that had migrated to the basal side of the membrane were fixed and stained with crystal violet, visualized and represent photos were taken under a 200–fold vision.

WESTERN BLOTTING

Proteins were separated by 10% SDS–PAGE and transferred to polyvinylidene fluoride (PVDF) membrane. The membrane was incubated with primary antibodies to E-cadherin (1:1,000, BD Biosciences), N-cadherin (1:1 000, BD Biosciences), Vimentin (1:1 000, BD Biosciences), CK-19 (1:1 000, BD Biosciences), and Twist (1:500, Santa Cruz Biotechnology, Inc.) overnight at 4°C and then incubated with HRP-conjugated secondary antibody for 1 h at 37°C. The results were photographed with ECL substrate (Cell signaling) according to the manufacture's instructions.

ANIMAL EXPERIMENTS

To investigate the migrate and invasive ability of SPC-A1/DTX cells in vivo, male BALB/c nude mice aged 6–8 weeks were purchased from the Animal Laboratory Unit of Jinling Hospital. The mice were maintained under standard conditions and cared for according to the institutional guidelines for animal care. SPC-A1 and SPC-A1/DTX cells were harvested and 6×10^6 viable cells were injected into the lateral tail vein of nude mice (twenty per group). After 8 weeks, blood from mice was isolated and red blood cells were lysed. The mRNA from the remaining cells was extracted for real-time PCR. At the same time, lung tissues were fixed by paraformaldehyde and alveolar structure was observed through H&E staining.

To explore the role of ZEB1 on the chemoresistance of SPC-A1/DTX cells, 48 h after transfection with sicon or siZEB1, SPC-A1/DTX cells (1×10^6) were suspended in 100 μl PBS and then injected subcutaneously into nude mice at the right side of the posterior flank, six mice per group. Tumor growth was examined every other day, and tumor volumes were calculated by using the equation $V = A \times B^2/2$ (mm^3), wherein A is the largest diameter, and B is the perpendicular diameter. When the average tumor size reached about 50 mm^3, docetaxel (1 mg/kg) was given every other day intraperitoneally. After 17 days, all mice were sacrificed. The animal study protocol was approved by the Animal Experimentation Ethics Committee of the Jinling Hospital.

STATISTICAL ANALYSIS

The results were expressed as mean ± SEM and analyzed by SPSS12.0 statistical analytical software (SPSS, Chicago, IL). Comparisons were carried out by Student's *t*-test and $P < 0.05$ were considered statistically significant.

RESULTS

ACQUISITION OF DOCETAXEL RESISTANCE INDUCES MORPHOLOGIC AND MOLECULAR CHANGES OF SPC-A1 CELLS CONSISTENT WITH EMT

We first determined the docetaxel resistant ability of SPC-A1/DTX cells. As shown in Figure 1A, the IC_{50} values of SPC-A1/DTX and SPC-A1 cells for docetaxel were 91.34 ± 3.30 and 8.48 ± 0.54 μg/L, respectively. And the IC_{50} values of SPC-A1/DTX and SPC-A1 cells for paclitaxel were 5.02 ± 0.55 and 0.65 ± 0.07 μg/L, respectively, which indicated that SPC-A1/DTX cells were also resistant to paclitaxel (Fig. 1B). SPC-A1/DTX cell line had a markedly different light microscopic appearance from the parental cell line. The phenotypic changes were observed in SPC-A1/DTX cells including loss of cell polarity, increased intercellular separation, and increased formation of pseudopodia (Fig. 1C), which were typical of cells with a mesenchymal phenotype. To further investigate whether the acquisition of docetaxel resistance induced specific molecular changes consistent with EMT, real-time PCR, and Western blotting were performed to detect the mRNA and protein expression of the EMT markers in SPC-A1/DTX and parental SPC-A1 cell line. As shown in Figure 1D–F, decreased mRNA and protein levels of the

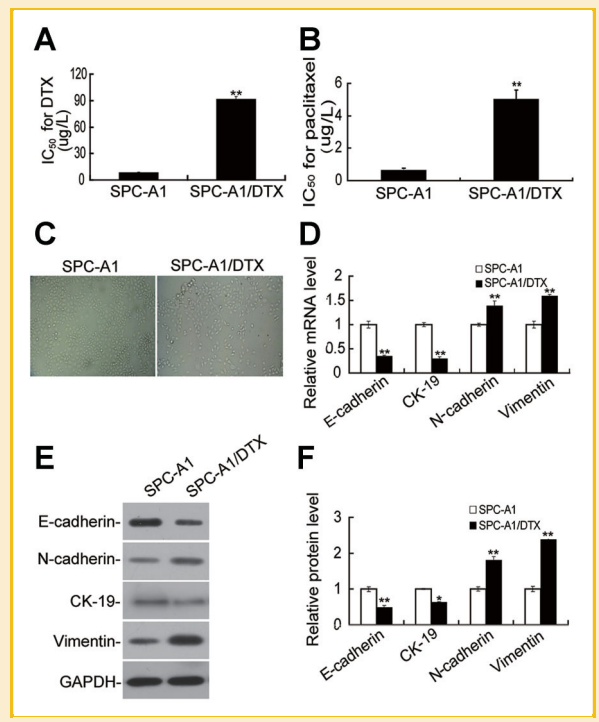

Fig. 1. SPC-A1/DTX cells exhibit EMT phenotype compared to parental SPC-A1 cells. A: IC_{50} values of SPC-A1/DTX and SPC-A1 cells for docetaxel. $^{**}P < 0.01$. B: IC_{50} values of SPC-A1/DTX and SPC-A1 cells for paclitaxel. $^{**}P < 0.01$. C: SPC-A1/DTX cells display phenotypic changes including a spindle-shaped morphology and increased formation of pseudopodia. Magnification, 100×. D: The expression of epithelial and mesenchymal markers was determined by real-time PCR in SPC-A1 and SPC-A1/DTX cells. $^{**}P < 0.01$. E: The expression of epithelial and mesenchymal markers was detected by Western blotting in SPC-A1 and SPC-A1/DTX cells. F: Quantitative analysis of the relative protein levels shown in E. $^{*}P < 0.05$, $^{**}P < 0.01$.

epithelial adhesion molecules such as E-cadherin and CK-19, and increased levels of mesenchymal markers such as Vimentin and N-cadherin were detected in SPC-A1/DTX cells compared with SPC-A1 cells. Interestingly, similar protein expression patterns were observed during the acquisition of docetaxel resistance in another human non-small cell lung carcinoma cell line, H1299, which suggested that docetaxel-induced EMT phenotype was not cell type specific (Supplementary Fig. 1).

SPC-A1/DTX CELL LINE HAS INCREASED MIGRATORY AND INVASIVE CAPACITY BOTH IN VITRO AND IN VIVO

The EMT program is associated with enhanced cancer invasiveness. Therefore, we next compared migratory ability and invasive potential between the SPC-A1/DTX and parental SPC-A1 cells. As shown in Figure 2A,B, the capacity of SPC-A1/DTX cell line to invade through the transwell membrane was 2.40-fold compared with that of the parental SPC-A1 cell line. In addition, the SPC-A1/DTX cells showed a 1.62- and 1.17-fold increase in the number of cells migrating across the wound at 24 and 48 h, respectively (Fig. 2C,D). Increased formation of pseudopodia was also observed in the edge of the wounds of SPC-A1/DTX cells compared to those of SPC-A1 cell line (Fig. 2C). Similar results were observed in H1299 cells during the acquisition of docetaxel resistance (Supplementary Fig. 2). The metastatic potential of SPC-A1/DTX cells was also investigated in vivo. As shown in Figure 2E, compared with the SPC-A1 cells injected nude mice, H&E staining showed that 8 weeks after injection of SPC-A1/DTX cells, numerous multinucleate huge cells, newly formed vessels, and scattered lymphocytes were seen in the lung sections and markedly more space in pulmonary alveolus was occupied by tumor cells. The number of circulating tumor cells was also significantly increased in SPC-A1/DTX cells injected mice ($P < 0.05$, Fig. 2F). These results suggested that SPC-A1/DTX cell line exerted increased migratory and invasive capacity both in vitro and in vivo.

DOWN-REGULATION OF ZEB1 LEADS TO THE REVERSAL OF EMT PHENOTYPE IN SPC-A1/DTX CELLS

To identify the transcription factors that were involved in the docetaxel-induced EMT phenotype, we analyzed expression levels of the following known EMT activators including Snail1, Snail2, Twist, ZEB1, and ZEB2. The expression levels of EMT activators such as Snail1, Snail2, and Twist, showed no significant changes at both transcriptional and translational levels (Fig. 3). ZEB2 was not detected at either the mRNA or protein level (data not shown). However, expression of ZEB1 in SPC-A1/DTX cell line was

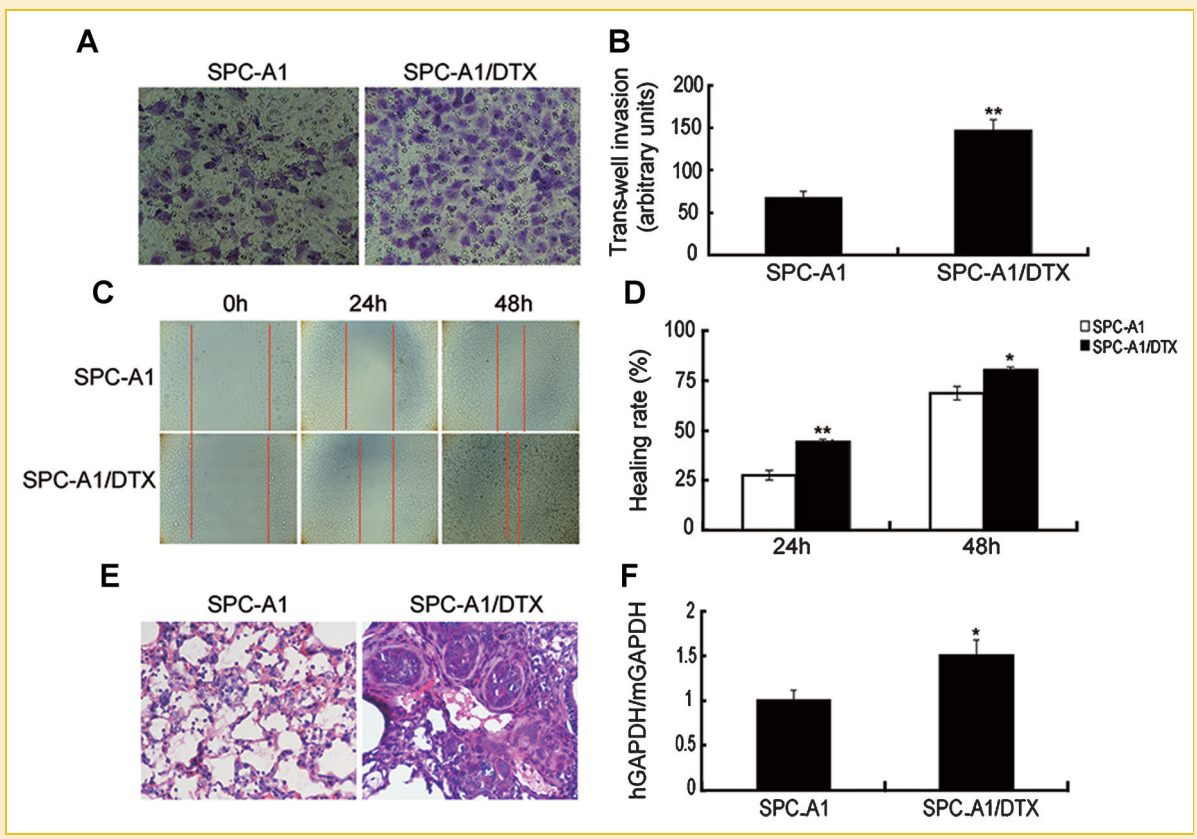

Fig. 2. SPC-A1/DTX cell line has increased migratory and invasive capacity both in vitro and in vivo. A: Cell migration capacity of SPC-A1 and SPC-A1/DTX cells was determined by transwell assay. B: Quantitative analysis of the cells migration through the transwell chambers. $^{**}P < 0.01$. C: Wound healing assays were performed at 24 and 48 h in SPC-A1 and SPC-A1/DTX cells. D: Quantitative analysis of the healing rate of SPC-A1 and SPC-A1/DTX cells. $^{*}P < 0.05$, $^{**}P < 0.01$. E: At 8 weeks after tail vein injection of SPC-A1 or SPC-A1/DTX cells, metastasis potential was determined by histological analysis using HE staining. F: The relative concentration of circulating tumor cells in blood was determined by real-time PCR. $^{*}P < 0.05$.

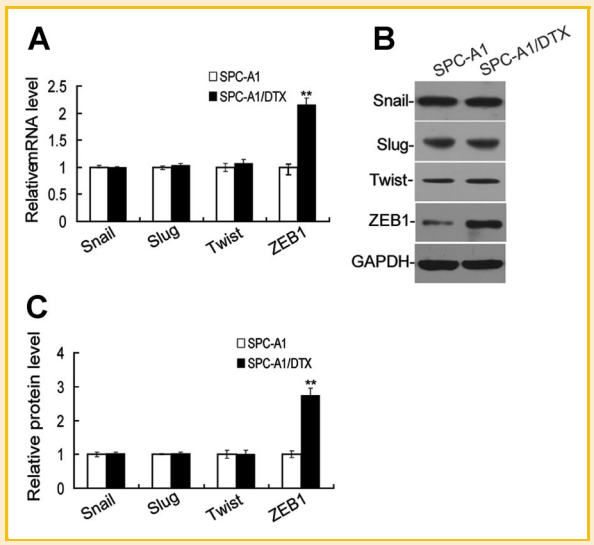

Fig. 3. ZEB1 was upregulated in SPC-A1/DTX cells. A: Expression levels of transcription factors Snail1, Snail2, Twist, and ZEB1 were determined by real-time PCR in SPC-A1 and SPC-A1/DTX cells. $^{**}P < 0.01$. B: Expression levels of transcription factors Snail1, Snail2, Twist, and ZEB1 were determined by Western blotting in SPC-A1 and SPC-A1/DTX cells. C: Quantitative analysis of the relative protein levels shown in B. $^{**}P < 0.01$.

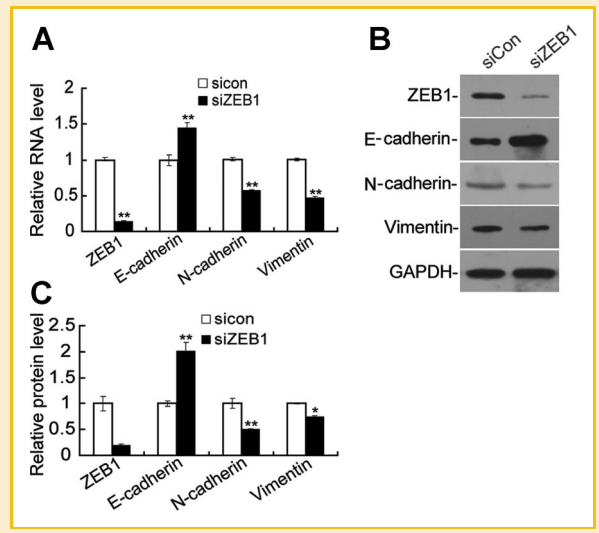

Fig. 4. RNAi-mediated knockdown of ZEB1 modulates the expression of EMT markers in SPC-A1/DTX cells. A: The RNA expression of ZEB1, E-cadherin, Vimentin, and N-cadherin was detected in SPC-A1/DTX cells following inhibition of ZEB1 by siZEB1. $^{*}P < 0.05$, $^{**}P < 0.01$. B: The protein expression of ZEB1, E-cadherin, Vimentin, and N-cadherin was detected in SPC-A1/DTX cells following inhibition of ZEB1 by siZEB1. C: Quantitative analysis of the relative protein levels shown in B. $^{*}P < 0.05$, $^{**}P < 0.01$.

significantly increased at both mRNA and protein levels (Fig. 3). To further determine the role of ZEB1 in the formation of EMT phenotype in SPC-A1/DTX cell line, siRNA specifically targeting ZEB1 was transfected into SPC-A1/DTX cells. As shown in Figure 4, inhibition of ZEB1 up-regulated the expression of E-cadherin and decreased the expression of Vimentin and N-cadherin. In addition, knockdown of ZEB1 significantly inhibited the migratory potential of SPC-A1/DTX cells in the transwell assay ($P < 0.01$, Fig. 5A,B). Furthermore, inhibition of ZEB1 resulted in a 43.7% and 44.0% decrease in the number of cells migrating across the wound at 24 and

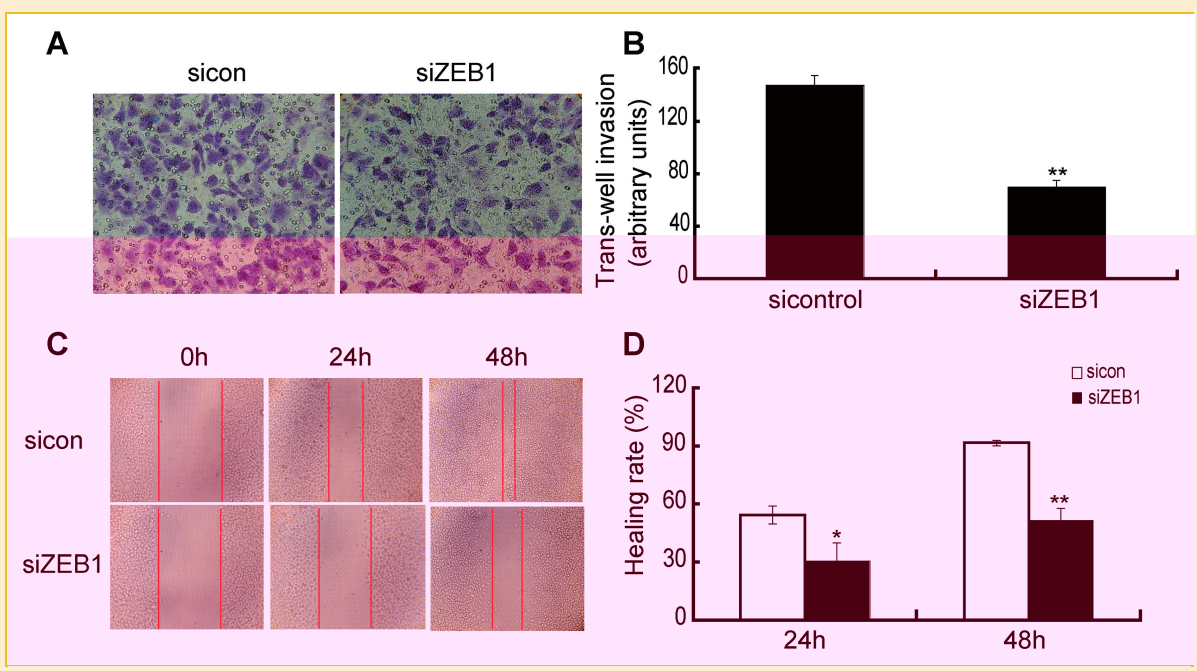

Fig. 5. Inhibition of ZEB1 decreased the migratory ability of SPC-A1/DTX cells. A: Cell migration capacity of siZEB1-transfected SPC-A1/DTX cells was determined by transwell assay. B: Quantitative analysis of the cells migrating through the transwell chambers. $^{**}P < 0.01$. C: Wound healing assays were performed at 24 and 48 h in siZEB1-transfected SPC-A1/DTX cells. D: Quantitative analysis of the healing rate of sicon-transfected and siZEB1-transfected SPC-A1/DTX cells. $^{*}P < 0.05$, $^{**}P < 0.01$.

48 h, respectively (Fig. 5C,D). All of these data indicated that ZEB1 was critical for the acquisition of EMT phenotype and that the inhibition of ZEB1 could reverse the EMT phenotype of docetaxel-resistant cells.

KNOCKDOWN OF ZEB1 ENHANCES THE CHEMOSENSITIVITY OF SPC-A1/DTX CELLS TO DOCETAXEL

Next we explored the role of ZEB1 on the chemosensitivity of SPC-A1/DTX cells to docetaxel. As shown in Figure 6A,B, inhibition of ZEB1 significantly suppressed proliferating ability of SPC-A1/DTX cells compared with sicon-transfected cells in the colony formation assay ($P < 0.01$). Moreover, down-regulation of ZEB1 could enhance the apoptotic rate of SPC-A1/DTX cells from $2.02 \pm 0.22\%$ to $5.99 \pm 0.44\%$ by flow cytometric analysis (Fig. 6C,D). Given that inhibition of ZEB1 could reverse the EMT phenotype of SPC-A1/DTX cells, we asked whether inhibition of ZEB1 could affect the chemosensitivity of SPC-A1/DTX cells. As shown in Figure 6E, the IC_{50} values for docetaxel were 102.72 ± 4.76 and 33.87 ± 3.48 μg/L in sicon- and siZEB1-transfected SPC-A1/DTX cells, respectively. And the IC_{50} values for paclitaxel were significantly decreased in siZEB1-transfected SPC-A1/DTX cells ($P < 0.01$, Fig. 6F). To investigate whether inhibiting of ZEB1 could reverse the docetaxel resistance of SPC-A1/DTX cells in vivo, siZEB1-transfected SPC-A1/DTX cells were injected subcutaneously into nude mice and docetaxel was given through intraperitoneal injection. As shown in Figure 6G,H, knockdown of ZEB1 could significantly decrease the tumor volume, which indicated that inhibiting of ZEB1 increased the docetaxel sensibility of the SPC-A1/DTX cells. All these results suggest

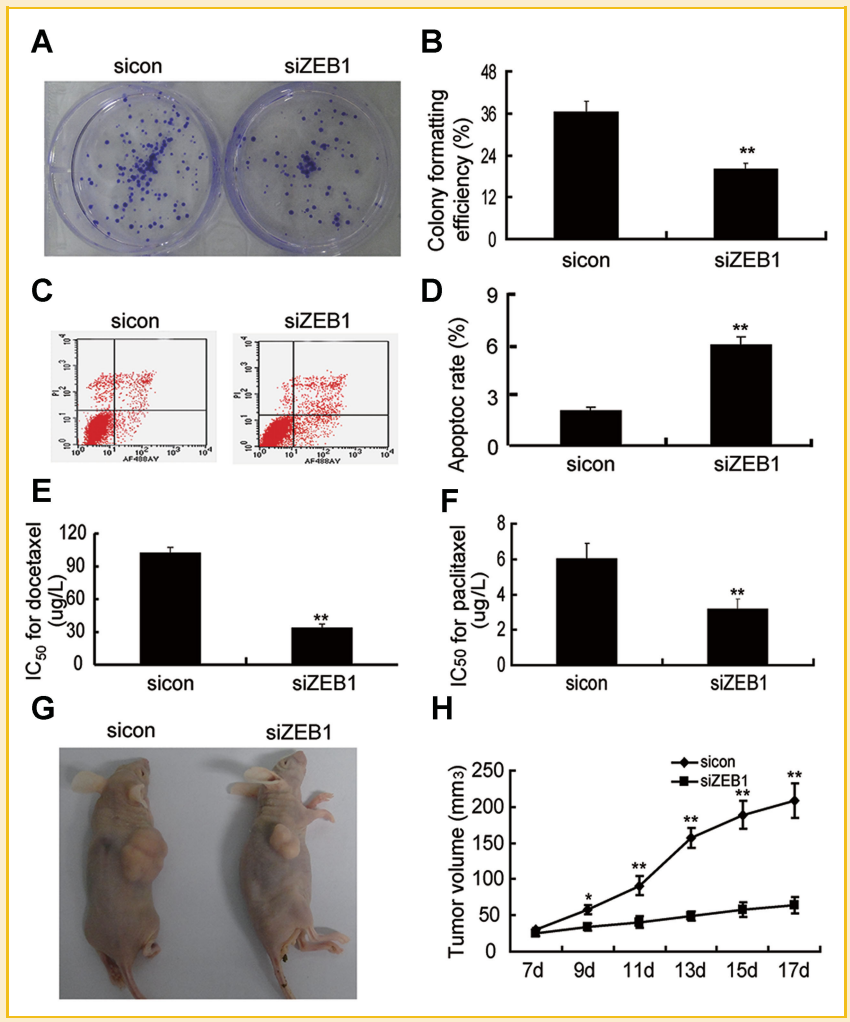

Fig. 6. Inhibition of ZEB1 increases the chemosensitivity of SPC-A1/DTX cells to docetaxel in vivo and in vitro. A: The proliferating ability of siZEB1-transfected SPC-A1/DTX cells was determined in the colony formatting assay. B: Quantitative analysis of the proliferating ability of siZEB1-transfected SPC-A1/DTX cells shown in A. $^{**}P < 0.01$. C: Apoptosis rate of siZEB1-transfected SPC-A1/DTX cells was detected by flow cytometry. D: Quantitative analysis of the apoptosis rate of siZEB1-transfected SPC-A1/DTX cells shown in C. $^{**}P < 0.01$. E: IC_{50} values of sicon-transfected and siZEB1-transfected SPC-A1/DTX cells for docetaxel. $^{**}P < 0.01$. F: IC_{50} values of sicon-transfected and siZEB1-transfected SPC-A1/DTX cells for paclitaxel. $^{**}P < 0.01$. G: Representative photographs of tumors formed at 17 days after the subcutaneous transplantation. H: Growth curve of tumors derived from sicon-transfected and siZEB1-transfected SPC-A1/DTX cells. $^{*}P < 0.05$, $^{**}P < 0.01$. n = 6 mice per group.

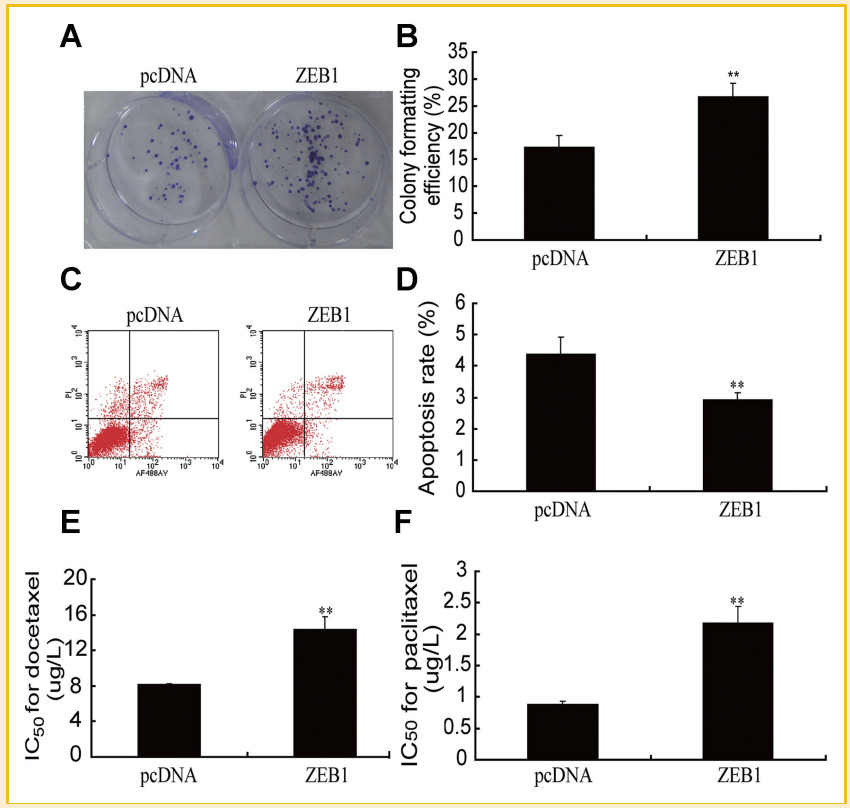

Fig. 7. Ectopic expression of ZEB1 decreases the chemosensitivity of SPC-A1 cells to docetaxel in vitro. A: The proliferating ability of ZEB1-transfected SPC-A1 cells was determined in the colony formatting assay. B: Quantitative analysis of the proliferating ability of ZEB1-transfected SPC-A1 cells shown in Figure 6A. $^{**}P < 0.01$. C: Apoptosis rate of ZEB1-transfected SPC-A1 cells was detected by flow cytometry. D: Quantitative analysis of the apoptosis rate of ZEB1-transfected SPC-A1 cells shown in C. $^{**}P < 0.01$. E: IC_{50} values of ZEB1-transfected SPC-A1 cells for docetaxel. $^{**}P < 0.01$. F: IC_{50} values of ZEB1-transfected SPC-A1 cells for paclitaxel. $^{**}P < 0.01$.

that inhibition of ZEB1 could enhance the docetaxel sensitivity of SPC-A1/DTX cells.

ECTOPIC EXPRESSION OF ZEB1 ATTENUATES THE CHEMOSENSITIVITY OF SPC-A1 CELLS TO DOCETAXEL

To further confirm the critical role of ZEB1 in chemosensitivity to docetaxel, ZEB1 was overexpressed in parental SPC-A1 cells. As shown in Figure 7A, the proliferating ability of SPC-A1 cells, which were transfected with ZEB1, was significantly increased compared with pcDNA-transfected cells ($P < 0.01$, Fig. 7A,B). In addition, ectopic expression of ZEB1 significantly decrease the apoptotic rate of SPC-A1 cells ($P < 0.01$, Fig. 7C,D). Furthermore, the IC_{50} values for docetaxel were significantly increased from 8.13 ± 0.16 to 14.38 ± 1.39 μg/L when transfected with ZEB1 ($P < 0.01$, Fig. 7E). The IC_{50} values for paclitaxel were also significantly increased in ZEB1-transfected SPC-A1 (Fig. 6F). Taken together, these results suggest that ZEB1 played an important role in the formation of docetaxel resistance in SPC-A1/DTX cells.

DISCUSSION

In this study, we have for the first time demonstrated that SPC-A1/DTX cells showed EMT characteristics including elongated fibroblastoid shape, switch of EMT marker proteins, and enhanced migratory and invasive potential. In addition, ZEB1 played a crucial role in the induction of EMT and chemosensitivity to docetaxel of SPC-A1 cells by targeting E-cadherin, suggesting that ZEB1 was a potential target for NSCLC treatment.

EMT was correlated with cancer cell metastasis as well as resistance towards anticancer agents [Gomes et al., 2011; Chen et al., 2012]. It was generally considered that cell phenotype was responsible for the sensitivity of therapeutic agents, which suggested that mesenchymal-type cancer cells were more resistant to chemotherapeutic agents than epithelial-type cancer cells [Fuchs et al., 2008; Maseki et al., 2012]. Further studies indicated that E-cadherin expression was a novel biomarker predicting clinical positive activity of the EGFR inhibitor erlotinib in NSCLC patients [Thomson et al., 2005; Uramoto et al., 2011]. Here, our study showed that docetaxel-resistant SPC-A1 cells exhibited EMT phenotype including loss of cell-to-cell contact, acquisition of fibroblast-like morphology, switch of EMT marker proteins and increased migratory abilities both in vitro and in vivo. Interestingly, in the xenograft nude mice models, there were no visible metastatic nodules in the lung in spite of increased number of circulating tumor cells, and we speculated that it was most likely due to the lower invasion and metastasis ability of SPC-A1 cells.

Several master EMT-regulating transcription factors, including Twist, Snail, Slug, ZEB1, SIP, and Goosecoid, played indispensable roles in epithelial cancers [Christiansen and Rajasekaran, 2006; Klymkowsky and Savagner, 2009]. Among them, Snail and Twist were shown to repress the expression of E-cadherin and induce EMT in cancer cells [Batlle et al., 2000; Cano et al., 2000]. Increased expression of Snail and Twist were often correlated with poor prognosis in hepatocellular, breast, colorectal, and gastric cancers [Miyoshi et al., 2005; Yan-Qi et al., 2007; Vesuna et al., 2008; Valdes-Mora et al., 2009]. More importantly, ZEB1 was regarded as a key player in the progression of epithelial cancers by targeting E-cadherin. ZEB1 was up-regulated in advanced stages of colorectal tumors and uterine cancers and enhanced transendothelial migration in prostate cancer cells [Schmalhofer et al., 2009]. ZEB1 was a critical transcription factor that repressed the expression of E-cadherin via binding to two bipartite E-box motifs within the E-cadherin promoter [Peinado et al., 2004]. Recently, it was reported that ZEB1 may be linked to the recruitment of histone deacetylases at the E-cadherin promoter [Tryndyak et al., 2010]. Consistent with these findings, we found that ZEB1 was up-regulated in SPC-A1/DTX cells compared to parental SPC-A1 cells and knockdown of ZEB1 induced up-regulation of E-cadherin and down-regulation of N-cadherin and Vimentin, and reduced migratory and invasive potential of SPC-A1/DTX cells.

It was generally accepted that the EMT process prevented apoptosis of cancer cells and induced resistance to chemotherapy. For example, Twist1 might contribute to the disruption of repressive complexes between p53 and p21, and depletion of Twist1 could raise the apoptotic rate of breast cancer cells and reverse the sensitivity to chemotherapy [Li et al., 2009]. Snail and Slug were also involved in resistance to paclitaxel, adriamycin, and radiation by inactivating p53-mediated apoptosis [Kajita et al., 2004; Kurrey et al., 2009]. Accumulating evidence has indicated that ZEB1 was associated with cell sensitivity to conventional chemotherapy, including gemcitabine, 5-fluorouracil (5-FU), and cisplatin in cancer cells [Arumugam et al., 2009]. In addition, the data have shown that knockdown of ZEB1 greatly suppressed anchorage-independent growth of lung cancer cells [Takeyama et al., 2010]. Based on this observation, we evaluated the effects of ZEB1 on resistance to docetaxel and proliferating ability in SPC-A1/DTX cell line. Intriguingly, inhibition of ZEB1 significantly enhanced the sensitivity of lung adenocarcinoma cells to docetaxel in vitro and in vivo. Meanwhile, inhibition of ZEB1 significantly inhibited proliferating ability and increased the apoptotic rate of SPC-A1/DTX cells, which indicated that ZEB1 was a critical determinant for docetaxel-resistance of lung adenocarcinoma cells. Furthermore, ectopic expression of ZEB1 could decrease the chemosensitivity to docetaxel in parental SPC-A1 cells. All these results suggested that suppression of ZEB1 would be a useful approach for the reversal of EMT and drug resistance phenotype of SPC-A1/DTX cells.

Resistance to chemotherapeutic agents represented a major obstacle for the treatment of patients with NSCLC and the presence of EMT phenotypic cells could take responsibility, at least partially, for the development of NSCLC chemoresistance and the high mortality of NSCLC patients. Our study demonstrated that inhibition of ZEB1 could up-regulate the expression of E-cadherin, resulted in the reversal of EMT characteristics and chemoresistance of SPC-A1/DTX cells, which provided new insights into further investigation in understanding the mechanism of ZEB1 in the drug resistance for the successful treatment of NSCLC.

REFERENCES

Aigner K, Dampier B, Descovich L, Mikula M, Sultan A, Schreiber M, Mikulits W, Brabletz T, Strand D, Obrist P, Sommergruber W, Schweifer N, Wernitznig A, Beug H, Foisner R, Eger A. 2007a. The transcription factor ZEB1 (deltaEF1) promotes tumour cell dedifferentiation by repressing master regulators of epithelial polarity. Oncogene 26:6979–6988.

Aigner K, Descovich L, Mikula M, Sultan A, Dampier B, Bonne S, van Roy F, Mikulits W, Schreiber M, Brabletz T, Sommergruber W, Schweifer N, Wernitznig A, Beug H, Foisner R, Eger A. 2007b. The transcription factor ZEB1 (deltaEF1) represses Plakophilin 3 during human cancer progression. FEBS Lett 581:1617–1624.

Arumugam T, Ramachandran V, Fournier KF, Wang H, Marquis L, Abbruzzese JL, Gallick GE, Logsdon CD, McConkey DJ, Choi W. 2009. Epithelial to mesenchymal transition contributes to drug resistance in pancreatic cancer. Cancer Res 69:5820–5828.

Barr S, Thomson S, Buck E, Russo S, Petti F, Sujka-Kwok I, Eyzaguirre A, Rosenfeld-Franklin M, Gibson NW, Miglarese M, Epstein D, Iwata KK, Haley JD. 2008. Bypassing cellular EGF receptor dependence through epithelial-to-mesenchymal-like transitions. Clin Exp Metastasis 25:685–693.

Batlle E, Sancho E, Franci C, Dominguez D, Monfar M, Baulida J, Garcia De Herreros A. 2000. The transcription factor snail is a repressor of E-cadherin gene expression in epithelial tumour cells. Nat Cell Biol 2:84–89.

Cano A, Perez-Moreno MA, Rodrigo I, Locascio A, Blanco MJ, del Barrio MG, Portillo F, Nieto MA. 2000. The transcription factor snail controls epithelial-mesenchymal transitions by repressing E-cadherin expression. Nat Cell Biol 2:76–83.

Chen X, Wang Y, Xia H, Wang Q, Jiang X, Lin Z, Ma Y, Yang Y, Hu M. 2012. Loss of E-cadherin promotes the growth, invasion and drug resistance of colorectal cancer cells and is associated with liver metastasis. Mol Biol Rep 39:6707–6714.

Christiansen JJ, Rajasekaran AK. 2006. Reassessing epithelial to mesenchymal transition as a prerequisite for carcinoma invasion and metastasis. Cancer Res 66:8319–8326.

Comijn J, Berx G, Vermassen P, Verschueren K, van Grunsven L, Bruyneel E, Mareel M, Huylebroeck D, van Roy F. 2001. The two-handed E box binding zinc finger protein SIP1 downregulates E-cadherin and induces invasion. Mol Cell 7:1267–1278.

Eger A, Aigner K, Sonderegger S, Dampier B, Oehler S, Schreiber M, Berx G, Cano A, Beug H, Foisner R. 2005. DeltaEF1 is a transcriptional repressor of E-cadherin and regulates epithelial plasticity in breast cancer cells. Oncogene 24:2375–2385.

Feng B, Wang R, Song HZ, Chen LB. 2011. MicroRNA-200b reverses chemoresistance of docetaxel-resistant human lung adenocarcinoma cells by targeting E2F3. Cancer 118:3365–3376.

Fuchs BC, Fujii T, Dorfman JD, Goodwin JM, Zhu AX, Lanuti M, Tanabe KK. 2008. Epithelial-to-mesenchymal transition and integrin-linked kinase mediate sensitivity to epidermal growth factor receptor inhibition in human hepatoma cells. Cancer Res 68:2391–2399.

Gomes LR, Terra LF, Sogayar MC, Labriola L. 2011. Epithelial-mesenchymal transition: Implications in cancer progression and metastasis. Curr Pharm Biotechnol 12:1881–1890.

Hiscox S, Jiang WG, Obermeier K, Taylor K, Morgan L, Burmi R, Barrow D, Nicholson RI. 2006. Tamoxifen resistance in MCF7 cells promotes EMT-like behaviour and involves modulation of beta-catenin phosphorylation. Int J Cancer 118:290–301.

Hugo H, Ackland ML, Blick T, Lawrence MG, Clements JA, Williams ED, Thompson EW. 2007. Epithelial–mesenchymal and mesenchymal–epithelial transitions in carcinoma progression. J Cell Physiol 213:374–383.

Jemal A, Siegel R, Ward E, Hao Y, Xu J, Murray T, Thun MJ. 2008. Cancer statistics, 2008. CA Cancer J Clin 58:71–96.

Kajita M, McClinic KN, Wade PA. 2004. Aberrant expression of the transcription factors snail and slug alters the response to genotoxic stress. Mol Cell Biol 24:7559–7566.

Kajiyama H, Shibata K, Terauchi M, Yamashita M, Ino K, Nawa A, Kikkawa F. 2007. Chemoresistance to paclitaxel induces epithelial-mesenchymal transition and enhances metastatic potential for epithelial ovarian carcinoma cells. Int J Oncol 31:277–283.

Klymkowsky MW, Savagner P. 2009. Epithelial-mesenchymal transition: A cancer researcher's conceptual friend and foe. Am J Pathol 174:1588–1593.

Kong D, Wang Z, Sarkar SH, Li Y, Banerjee S, Saliganan A, Kim HR, Cher ML, Sarkar FH. 2008. Platelet-derived growth factor-D overexpression contributes to epithelial-mesenchymal transition of PC3 prostate cancer cells. Stem Cells 26:1425–1435.

Kurrey NK, Jalgaonkar SP, Joglekar AV, Ghanate AD, Chaskar PD, Doiphode RY, Bapat SA. 2009. Snail and slug mediate radioresistance and chemoresistance by antagonizing p53-mediated apoptosis and acquiring a stem-like phenotype in ovarian cancer cells. Stem Cells 27:2059–2068.

Larue L, Bellacosa A. 2005. Epithelial-mesenchymal transition in development and cancer: Role of phosphatidylinositol 3′ kinase/AKT pathways. Oncogene 24:7443–7454.

Li QQ, Xu JD, Wang WJ, Cao XX, Chen Q, Tang F, Chen ZQ, Liu XP, Xu ZD. 2009. Twist1-mediated adriamycin-induced epithelial-mesenchymal transition relates to multidrug resistance and invasive potential in breast cancer cells. Clin Cancer Res 15:2657–2665.

Maseki S, Ijichi K, Tanaka H, Fujii M, Hasegawa Y, Ogawa T, Murakami S, Kondo E, Nakanishi H. 2012. Acquisition of EMT phenotype in the gefitinib-resistant cells of a head and neck squamous cell carcinoma cell line through Akt/GSK-3beta/snail signalling pathway. Br J Cancer 106:1196–1204.

Mejlvang J, Kriajevska M, Vandewalle C, Chernova T, Sayan AE, Berx G, Mellon JK, Tulchinsky E. 2007. Direct repression of cyclin D1 by SIP1 attenuates cell cycle progression in cells undergoing an epithelial mesenchymal transition. Mol Biol Cell 18:4615–4624.

Min C, Eddy SF, Sherr DH, Sonenshein GE. 2008. NF-kappaB and epithelial to mesenchymal transition of cancer. J Cell Biochem 104:733–744.

Miyoshi A, Kitajima Y, Kido S, Shimonishi T, Matsuyama S, Kitahara K, Miyazaki K. 2005. Snail accelerates cancer invasion by upregulating MMP expression and is associated with poor prognosis of hepatocellular carcinoma. Br J Cancer 92:252–258.

Parkin DM, Bray F, Ferlay J, Pisani P. 2005. Global cancer statistics, 2002. CA Cancer J Clin 55:74–108.

Peinado H, Portillo F, Cano A. 2004. Transcriptional regulation of cadherins during development and carcinogenesis. Int J Dev Biol 48:365–375.

Peinado H, Olmeda D, Cano A. 2007. Snail, Zeb and bHLH factors in tumour progression: An alliance against the epithelial phenotype? Nat Rev Cancer 7:415–428.

Pena C, Garcia JM, Silva J, Garcia V, Rodriguez R, Alonso I, Millan I, Salas C, de Herreros AG, Munoz A, Bonilla F. 2005. E-cadherin and vitamin D receptor regulation by SNAIL and ZEB1 in colon cancer: Clinicopathological correlations. Hum Mol Genet 14:3361–3370.

Sabbah M, Emami S, Redeuilh G, Julien S, Prevost G, Zimber A, Ouelaa R, Bracke M, De Wever O, Gespach C. 2008. Molecular signature and therapeutic perspective of the epithelial-to-mesenchymal transitions in epithelial cancers. Drug Resist Updat 11:123–151.

Schmalhofer O, Brabletz S, Brabletz T. 2009. E-cadherin, beta-catenin, and ZEB1 in malignant progression of cancer. Cancer Metastasis Rev 28:151–166.

Shirakihara T, Saitoh M, Miyazono K. 2007. Differential regulation of epithelial and mesenchymal markers by deltaEF1 proteins in epithelial mesenchymal transition induced by TGF-beta. Mol Biol Cell 18:3533–3544.

Spaderna S, Schmalhofer O, Wahlbuhl M, Dimmler A, Bauer K, Sultan A, Hlubek F, Jung A, Strand D, Eger A, Kirchner T, Behrens J, Brabletz T. 2008. The transcriptional repressor ZEB1 promotes metastasis and loss of cell polarity in cancer. Cancer Res 68:537–544.

Takeyama Y, Sato M, Horio M, Hase T, Yoshida K, Yokoyama T, Nakashima H, Hashimoto N, Sekido Y, Gazdar AF, Minna JD, Kondo M, Hasegawa Y. 2010. Knockdown of ZEB1, a master epithelial-to-mesenchymal transition (EMT) gene, suppresses anchorage-independent cell growth of lung cancer cells. Cancer Lett 296:216–224.

Thomson S, Buck E, Petti F, Griffin G, Brown E, Ramnarine N, Iwata KK, Gibson N, Haley JD. 2005. Epithelial to mesenchymal transition is a determinant of sensitivity of non-small-cell lung carcinoma cell lines and xenografts to epidermal growth factor receptor inhibition. Cancer Res 65:9455–9462.

Tryndyak VP, Beland FA, Pogribny IP. 2010. E-cadherin transcriptional down-regulation by epigenetic and microRNA-200 family alterations is related to mesenchymal and drug-resistant phenotypes in human breast cancer cells. Int J Cancer 126:2575–2583.

Tsang WP, Kwok TT. 2009. The miR-18a* microRNA functions as a potential tumor suppressor by targeting on K-Ras. Carcinogenesis 30:953–959.

Uramoto H, Shimokawa H, Hanagiri T, Kuwano M, Ono M. 2011. Expression of selected gene for acquired drug resistance to EGFR-TKI in lung adenocarcinoma. Lung Cancer 73:361–365.

Valdes-Mora F, Gomez del Pulgar T, Bandres E, Cejas P, Ramirez de Molina A, Perez-Palacios R, Gallego-Ortega D, Garcia-Cabezas MA, Casado E, Larrauri J, Nistal M, Gonzalez-Baron M, Garcia-Foncillas J, Lacal JC. 2009. TWIST1 overexpression is associated with nodal invasion and male sex in primary colorectal cancer. Ann Surg Oncol 16:78–87.

Vandewalle C, Comijn J, De Craene B, Vermassen P, Bruyneel E, Andersen H, Tulchinsky E, Van Roy F, Berx G. 2005. SIP1/ZEB2 induces EMT by repressing genes of different epithelial cell-cell junctions. Nucleic Acids Res 33:6566–6578.

Vesuna F, van Diest P, Chen JH, Raman V. 2008. Twist is a transcriptional repressor of E-cadherin gene expression in breast cancer. Biochem Biophys Res Commun 367:235–241.

Wang TH, Wang HS, Soong YK. 2000. Paclitaxel-induced cell death: Where the cell cycle and apoptosis come together. Cancer 88:2619–2628.

Wu WS, Heinrichs S, Xu D, Garrison SP, Zambetti GP, Adams JM, Look AT. 2005. Slug antagonizes p53-mediated apoptosis of hematopoietic progenitors by repressing puma. Cell 123:641–653.

Yang J, Mani SA, Donaher JL, Ramaswamy S, Itzykson RA, Come C, Savagner P, Gitelman I, Richardson A, Weinberg RA. 2004. Twist, a master regulator of morphogenesis, plays an essential role in tumor metastasis. Cell 117:927–939.

Yang AD, Fan F, Camp ER, van Buren G, Liu W, Somcio R, Gray MJ, Cheng H, Hoff PM, Ellis LM. 2006. Chronic oxaliplatin resistance induces epithelial-to-mesenchymal transition in colorectal cancer cell lines. Clin Cancer Res 12:4147–4153.

Yan-Qi Z, Xue-Yan G, Shuang H, Yu C, Fu-Lin G, Fei-Hu B, Shi-Ren S, Xu-Feng W, Jie D, Dai-Ming F. 2007. Expression and significance of TWIST basic helix-loop-helix protein over-expression in gastric cancer. Pathology 39: 470–475.

Yu H. 2002. Regulation of APC-Cdc20 by the spindle checkpoint. Curr Opin Cell Biol 14:706–714.